
Absorption edge of $\text{Sn}(\text{Pb})_2\text{P}_2\text{S}(\text{Se})_6$ crystals under hydrostatic pressure

A.G.Slivka

Uzhhorod National University, Faculty of Physics, Voloshyn St. 32, Uzhhorod, 88000, Ukraine e-mail: optics@univ.uzhgorod.ua

Received 17.09.2001

Abstract

The experimental studies of hydrostatic pressure effect upon fundamental optical absorption spectra in $\text{Sn}(\text{Pb})_2\text{P}_2\text{S}(\text{Se})_6$ mixed crystals of different composition are carried out. The increase of Pb content in $(\text{Pb}_y\text{Sn}_{1-y})_2\text{P}_2\text{S}_6$, $(\text{Pb}_y\text{Sn}_{1-y})_2\text{P}_2\text{Se}_6$ crystals is shown to result in the enhancement of electron-phonon interaction and to the reduction of the energy gap deformation potential D_g . Isomorphous substitution of S by Se in the $\text{Sn}_2\text{P}_2(\text{S}_x\text{S}_{1-x})_6$ solid solution row does not affect significantly the electron-phonon interaction value and D_g .

Key words: Urbach absorption edge, ferroelectrics, phase transitions, hydrostatic pressure

PACS: 78.50.Ge, 77.80.Bh, 64.70.Rh

Introduction

Investigations of optical absorption spectra of $\text{Sn}_2\text{P}_2\text{S}_6$ -type crystals and relevant solid solutions at atmospheric pressure [1-6] have shown the spectral dependences of the absorption coefficient $\alpha(h\nu)$ to be of exponential character and to obey the Urbach rule

$$\alpha = \alpha_0 \exp[\sigma(h\nu - E_0)/kT]. \quad (1)$$

It was shown that in these crystals strong electron-phonon interaction exists and at ferroelectric phase transition all three parameters in Eq. (1) – α_0, E_0, σ_0 – are changed. According to [6], the exponential shape of the fundamental absorption edge in $\text{Sn}(\text{Pb})_2\text{P}_2\text{S}(\text{Se})_6$ crystals results from the interaction of the electron subsystems with phonons of deformational vibrations of $[\text{P}_2\text{S}(\text{Se})_6]^{4-}$ complex anions. Isomorphous

substitution in the cation sublattice ($\text{Sn} \rightarrow \text{Pb}$) in $\text{Sn}_2\text{P}_2\text{S}_6$ crystal increases the energy gap and enhances the electron-phonon interaction. Substitution in anion sublattice ($\text{S} \rightarrow \text{Se}$) decreases the energy gap and makes no essential effect upon the electron-phonon interaction value [6].

The present paper is aimed at studying the effect of external hydrostatic pressure on fundamental optical absorption spectra in mixed $\text{Sn}(\text{Pb})_2\text{P}_2\text{S}(\text{Se})_6$ crystals of various composition and determination of the contribution of the electron-phonon interaction into the temperature variation of the energy gap.

Experimental

Optical absorption studies were performed for 50-100 μm -thick single crystals, obtained by the chemical vapour transport method [7]. The spectral dependences of the absorption

coefficient α were obtained from the experimental studies of transmittance $T(h\nu)$ and reflectance $r(h\nu)$ spectra:

$$\alpha = (1/d) \ln \left\{ \frac{(1-r)^2 + \sqrt{(1-r)^4 + 4T^2 r^2}}{2T} \right\},$$

where d is the sample thickness. The spectral resolution of the optical setup on the base of MDR-2 monochromator was $1 \cdot 10^{-3}$ eV. The studies were carried out in polarized light ($\vec{E} \uparrow \uparrow \vec{b}$) in the high-pressure optical chamber [8].

Results and discussion

Figures 1–5 present the spectral dependences of the absorption coefficient $\alpha(h\nu)$ for $(\text{Pb}_y\text{Sn}_{1-y})_2\text{P}_2(\text{Se}_x\text{S}_{1-x})_6$ crystals in semilogarithmic scale at various external pressure values and the temperature $T = 296$ K. For all solid solution compositions hydrostatic pressure results in the absorption edge shift towards longer wavelengths, indicating the energy gap shrinking. In the insets to Figs. 1–5 the pressure dependences

of the absorption edge energy position $E_g^\alpha(p)$ for the absorption level of $\alpha = 150 \text{ cm}^{-1}$ are shown, as well as the pressure dependences of the characteristic energy $W = \frac{\Delta h\nu}{\Delta \ln \alpha} = \frac{kT}{\sigma}$, characterizing the spectral slope of the absorption edge and is the measure of the crystal disordering. In accordance with [9], the total value of the characteristic energy W for solid solutions can be given by

$$W = W_T + W_X = D_g [\langle u^2 \rangle_T + \langle u^2 \rangle_X], \quad (2)$$

where W_T determines the temperature-related disordering value, W_X – structural (topological) disordering, D_g – deformation potential for the characteristic energy, $\langle u^2 \rangle_T$ – mean-square deviation of the atoms from their ideal location in the crystal lattice due to the temperature-related disordering; $\langle u^2 \rangle_X$ – the similar value for the structural disordering.

The temperature and pressure dependences of the absorption edge energy position,

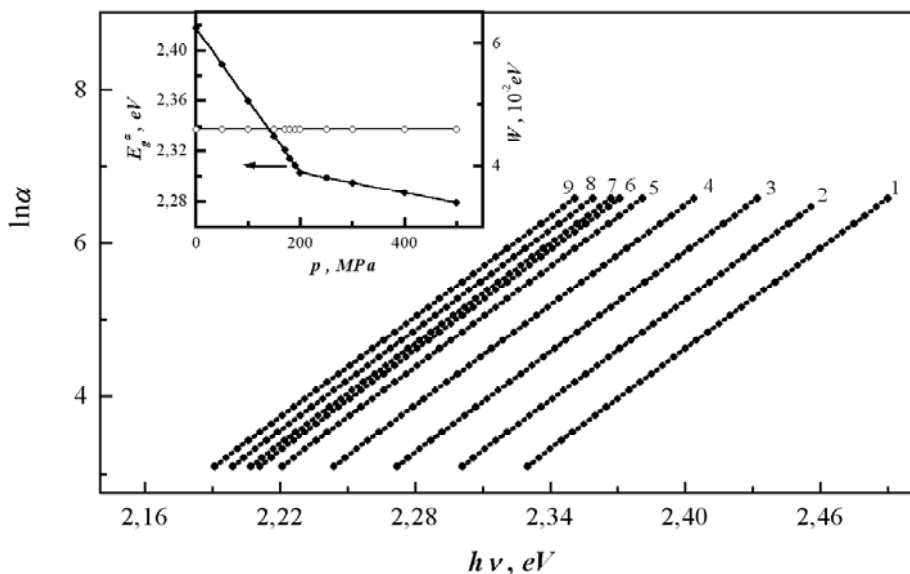


Fig.1. The spectral plots of the absorption coefficient logarithm for $\text{Sn}_2\text{P}_2\text{S}_6$ crystals of different pressures p , MPa: 1- 5; 2- 50; 3- 100; 4- 150; 5- 190; 6- 250; 7- 300; 8- 400; 9- 500. The insert shows the pressure dependences of the absorption edge energy position E_g^α and the Urbach characteristic energy W .

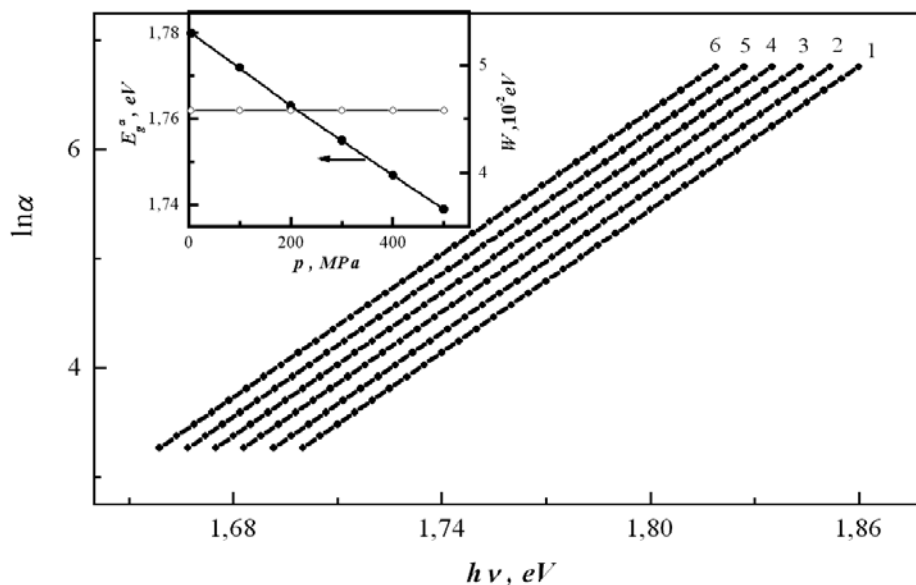


Fig.2. The spectral plots of the absorption coefficient logarithm for $\text{Sn}_2\text{P}_2\text{S}_6$ crystals of different pressures p , MPa: 1- 5; 2- 100; 3- 200; 4- 300; 5- 400; 6- 500. The insert shows the pressure dependences of the absorption edge energy position E_g^α and the Urbach characteristic energy W .

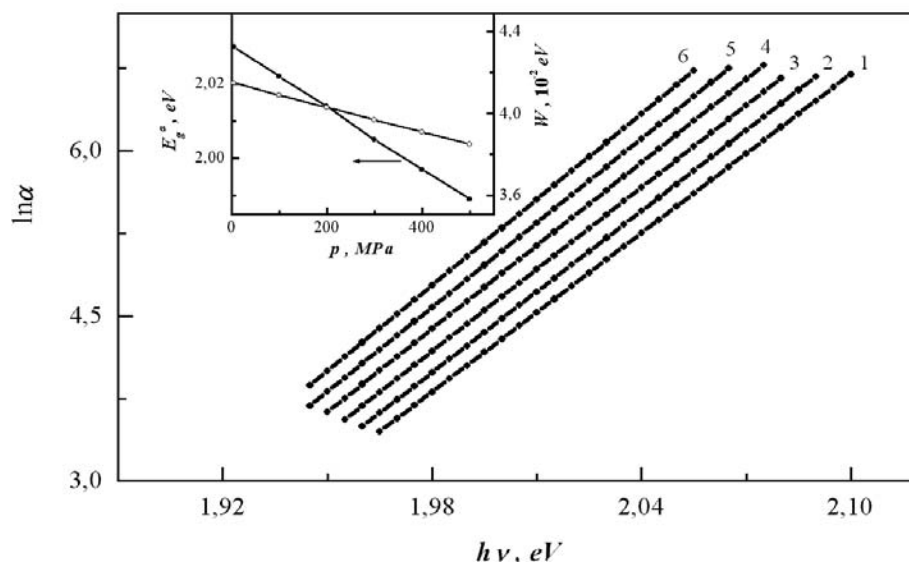


Fig.3. The spectral plots of the absorption coefficient logarithm for $\text{Sn}_2\text{P}_2(\text{Se}_{0.3}\text{S}_{0.7})_6$ crystals of different pressures p , MPa: 1- 5; 2- 100; 3- 200; 4- 300; 5- 400; 6- 500. The insert shows the pressure dependences of the absorption edge energy position E_g^α and the Urbach characteristic energy W .

described by Eq.(1), can be given by

$$E_g^\alpha(T, p) = E_0(p) - \frac{kT}{\sigma(T, p)} \ln\left(\frac{\alpha_0(p)}{\alpha}\right) = E_0(p) - W(T, p) \ln\left(\frac{\alpha_0(p)}{\alpha}\right) \quad (3)$$

The temperature dependence of E_g^α value at constant pressure is given solely by the temperature variation of the characteristic energy W . Meanwhile, the pressure dependence

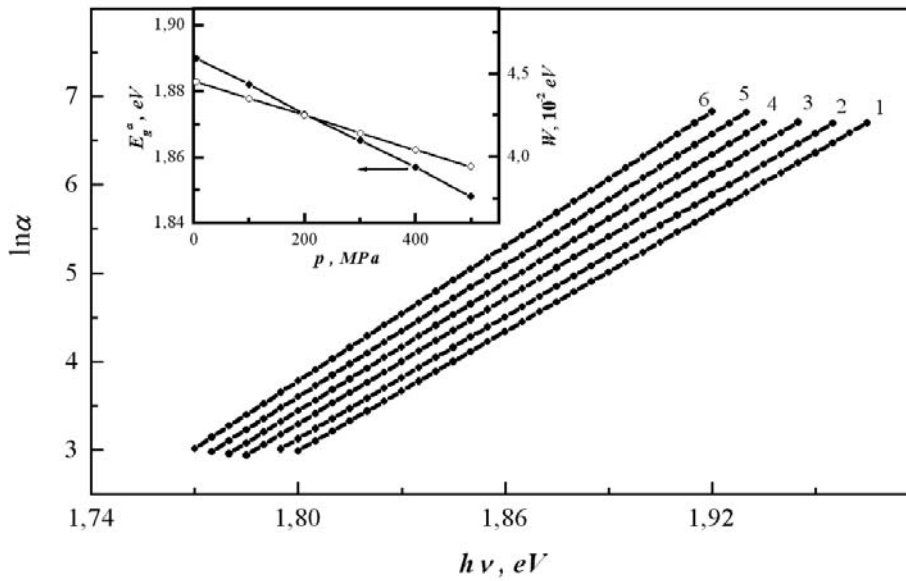


Fig.4. The spectral plots of the absorption coefficient logarithm for $\text{Sn}_2\text{P}_2(\text{Se}_{0.6}\text{S}_{0.4})_6$ crystals of different pressures p , MPa: 1- 5; 2- 100; 3- 200; 4- 300; 5- 400; 6- 500. The insert shows the pressure dependences of the absorption edge energy position E_g^α and the Urbach characteristic energy W .

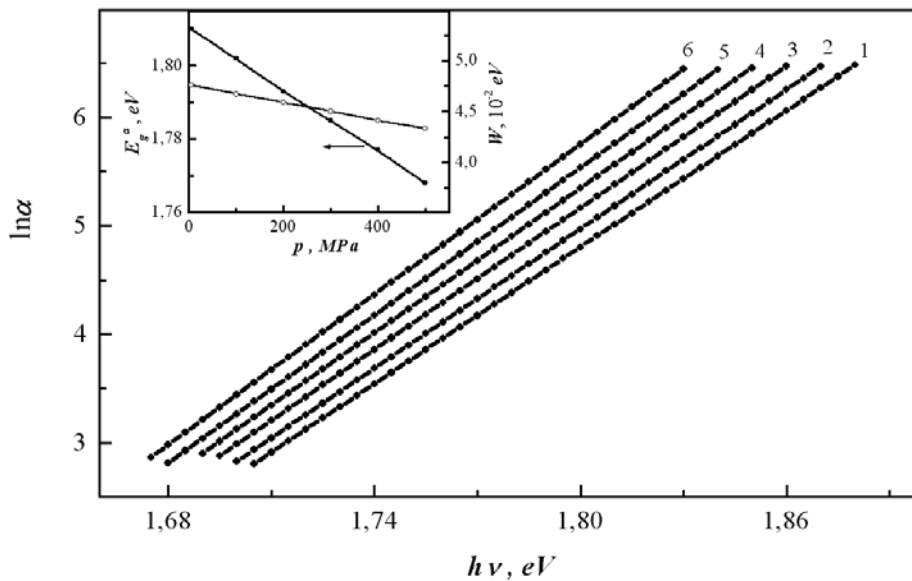


Fig.5. The spectral plots of the absorption coefficient logarithm for $\text{Sn}_2\text{P}_2(\text{Se}_{0.8}\text{S}_{0.2})_6$ crystals of different pressures p , MPa: 1- 5; 2- 100; 3- 200; 4- 300; 5- 400; 6- 500. The insert shows the pressure dependences of the absorption edge energy position E_g^α and the Urbach characteristic energy W .

of E_g^α value at constant temperature can result from both pressure variation of W value and variation of the Urbach relation parameters E_0 and α_0 . The pressure dependences of W, E_0, α_0

values within the same phase in the linear approximation can be given by

$$\begin{aligned} \alpha_0(p) &= \alpha_0(0) + a_0 \cdot p; \\ E_0(p) &= E_0(0) + b_0 \cdot p; \\ W(T, p) &= W(T, 0) + c_0 \cdot p. \end{aligned} \quad (4)$$

In $\text{Sn}_2\text{P}_2\text{S}_6$ and $\text{Sn}_2\text{P}_2\text{Se}_6$ crystals the absorption edge shifts with external pressure, this indicating the constant value of the characteristic energy W . Within the paraelectric phase α_0 value is also independent of the external pressure. Therefore, the pressure behaviour of the edge in these crystals is totally determined by the $E_0(p)$ dependence. This is confirmed by the equality of the coefficients $\frac{\partial E_g^\alpha}{\partial p} = \frac{\partial E_0}{\partial p}$. In $\text{Sn}_2\text{P}_2(\text{Sc}_x\text{S}_{1-x})_6$ mixed crystals at $x = 0.30; 0.60; 0.80$, contrary to the pure crystals, the decrease of the W value with pressure is observed experimentally. This indicates that in these solid solutions pressure results in the structural ordering of the crystals. The pressure coefficient of the characteristic energy value $c_0 = \partial W / \partial p$ in the paraelectric phase of $\text{Sn}_2\text{P}_2(\text{Sc}_x\text{S}_{1-x})_6$ crystals is: for $x = 0,30 - c_0 = -6,06 \cdot 10^{-3}$ eV/GPa; for $x = 0,60 - c_0 = -10,23 \cdot 10^{-3}$ eV/GPa; for $x = 0,80 - c_0 = -8,69 \cdot 10^{-3}$ eV/GPa. The b_0 coefficient value, representing the linear variation of the E_0 parameter under pressure, is -0.388 eV/GPa; -0.532 eV/GPa; -0.440 eV/GPa, for the crystals with $x = 0,30; 0,60; 0,80$, respectively. Besides the decrease of the W and

E_0 parameters for $\text{Sn}_2\text{P}_2(\text{Sc}_{0,30}\text{S}_{0,70})_6$ crystal the α_0 parameter decrease is experimentally observed. At atmospheric pressure the coordinates of $\ln \alpha_0(h\nu)$ plot convergency point for various temperatures in this crystal are $\alpha_0 = 2,680 \cdot 10^6 \text{ cm}^{-1}$ and $E_0 = 2,495$ eV, and at the pressure $p = 500$ MPa – $\alpha_0 = 0,361 \cdot 10^6 \text{ cm}^{-1}$ and $E_0 = 2,301$ eV. Thus, in this solid solution under external hydrostatic pressure, all the three parameters of the Urbach relation decrease, therefore the pressure variation of E_g^α is the general result of these changes.

In $\text{Sn}_2\text{P}_2(\text{Sc}_x\text{S}_{1-x})_6$ crystals with $x = 0; 0,10; 0,20$ and in $(\text{Pb}_y\text{Sn}_{1-y})_2\text{P}_2\text{S}_6$ crystals with $y = 0,05; 0,10$ at the temperature $T = 296$ K the increase of the external pressure results in the phase transition from the ferroelectric to the paraelectric phase [5,10]. This results in the change of the pressure coefficient dE_g^α / dp at the pressure, corresponding to the phase transition. In Table 1 temperature and pressure coefficients of E_g^α variation in different phases of crystals with a second-order phase transition are given. As known, the energy gap E_g can be expressed as an expansion over the phase transition order parameter:

Table 1.

Temperature and pressure coefficients of E_g^α variation and pressure coefficient of the phase transition temperature for $\text{Sn}(\text{Pb})_2\text{P}_2\text{S}(\text{Se})_6$ crystals

$x(y)$	$-\frac{dE_g^\alpha}{dT}$, 10^{-3} eV/K		$-\frac{dE_g^\alpha}{dp}$, 10^{-2} eV/GPa		$-\Delta\left(\frac{dE_g^\alpha}{dT}\right)$, 10^{-3} eV/K	$-\Delta\left(\frac{dE_g^\alpha}{dp}\right)$, 10^{-2} eV/GPa	$-dT_0 / dp$, K/GPa
	PE	FE	PE	FE			
$\text{Sn}_2\text{P}_2(\text{Sc}_x\text{S}_{1-x})_6$							
0	0,58	2,67	8,0	57,6	2,09	49,6	237
0,10	0,62	2,86	8,0	62,1	2,24	54,1	242
0,20	0,63	3,06	7,6	68,0	2,43	60,4	249
$(\text{Pb}_y\text{Sn}_{1-y})_2\text{P}_2\text{S}_6$							
0,05	0,70	2,27	7,5	45,5	1,57	38,0	242
0,10	0,68	1,54	7,8	29,5	0,86	21,7	252

$$E_g = E_{g0} + A\eta^2 + B\eta^4 + C\eta^6, \quad (5)$$

where E_{g0} is the energy gap in the paraelectric phase; A, B, C – expansion coefficients, being the parameters of the material. At the second-order phase transition the step $\Delta E_g = 0$, but the steps of the temperature and pressure coefficients $\Delta(dE_g/dT)_p$ and $\Delta(dE_g/dp)_T$ are observed [11]:

$$\begin{aligned} \Delta(dE_g/dT)_p &= -A \frac{\alpha_T}{\beta}, \\ \Delta(dE_g/dp)_T &= A \frac{\alpha_T}{\beta} \frac{dT_0}{dp}. \end{aligned} \quad (6)$$

where α_T, β are the coefficients of the thermodynamic potential expansion over the order parameter η , and dT_0/dp is the pressure coefficient of the phase transition temperature. It follows from Eq. (6) that

$$\frac{dT_0}{dp} = -\Delta\left(\frac{dE_g}{dp}\right)_T \times \left[\Delta\left(\frac{dE_g}{dT}\right)_p\right]^{-1}. \quad (7)$$

This relation enables the dT_0/dp value to be calculated from the experimental studies of the temperature and pressure behaviour of the fundamental absorption edge. The values of $\Delta(dE_g/dT)_p$ and $\Delta(dE_g/dp)_T$ as well as dT_0/dp coefficients, calculated according to Eq. (7) for various compositions of the solid solutions with the second-order phase transition are listed in Table 2. The obtained dT_0/dp values are in good agreement with the results of direct experimental studies of the p, T – phase diagrams [5,10].

Using the experimentally determined $\frac{dE_g^\alpha}{dp}$ coefficient values and bulk compressibility χ_V [12], we have calculated the values of the deformation potential of the energy gap

$$D_g = \frac{1}{\chi_V} \frac{dE_g^\alpha}{dp} \quad \text{for various solid solution}$$

compositions (See Table 2). The increase of Pb content in the $(\text{Pb}_y\text{Sn}_{1-y})_2\text{P}_2\text{S}_6$ and $(\text{Pb}_y\text{Sn}_{1-y})_2\text{P}_2\text{Se}_6$ solid solutions results in the decrease of the D_g value. The isomorphous substitution of S by Se does not lead to any essential changes in the D_g value.

To evaluate the contribution of the electron-phonon interaction into the temperature variation of the energy gap E_g^α we use the known relationship:

$$\left[\frac{dE_g^\alpha}{dT}\right]_p = \left[\frac{dE_g^\alpha}{dT}\right]_V - \frac{\alpha_V}{\chi_V} \left[\frac{dE_g^\alpha}{dp}\right]_T, \quad (8)$$

where α_V is the thermal coefficient of bulk expansion. The first term on the right-hand side of Eq. (8) characterizes the contribution of the temperature-related disordering of the structure into the variation of E_g^α due to the electron-phonon coupling. The second term represents the variation of E_g^α due to the variation of the crystal geometrical size. Based on the results of investigation of temperature and pressure behaviour of fundamental absorption edge of $\text{Sn}(\text{Pb})_2\text{P}_2\text{S}(\text{Se})_6$ crystals with the account of compositional dependences of χ_V and α_V , the

values of $\left[\frac{dE_g^\alpha}{dT}\right]_V$ and $\frac{\alpha_V}{\chi_V} \left[\frac{dE_g^\alpha}{dp}\right]_T$ were

calculated for the crystals of various composition (See Table 2). The second term in Eq. (8) is seen to be almost by an order of magnitude less than the first one. Hence, the decrease of E_g^α with temperature in the crystals under investigation is mostly due to the electron-phonon interaction. The increase of the

coefficient $m = \left[\frac{dE_g^\alpha}{dT}\right]_V \cdot \left(\frac{\alpha_V}{\chi_V} \left[\frac{dE_g^\alpha}{dp}\right]_T\right)^{-1}$

value with Pb concentration in $(\text{Pb}_y\text{Sn}_{1-y})_2\text{P}_2\text{S}_6$ and $(\text{Pb}_y\text{Sn}_{1-y})_2\text{P}_2\text{Se}_6$ crystals is the evidence for the increase of the electron-phonon interaction in these solid solutions. Substitution of S by Se

Table 2.

The values of $\left[\frac{dE_g^\alpha}{dT} \right]_V$, $\frac{\alpha_V}{\chi_V} \left[\frac{dE_g^\alpha}{dp} \right]_T$ parameters, deformational potential D_g and coefficient m for $\text{Sn}(\text{Pb})_2\text{P}_2\text{S}(\text{Se})_6$ mixed crystals.

Parameter	$y(x)$	$\left(\frac{dE_g^\alpha}{dT} \right)_V, 10^{-4}$ eV/K	$\frac{\alpha_V}{\chi_V} \left(\frac{dE_g^\alpha}{dp} \right)_T, 10^{-4}$ eV/K	$-D_g$, eV	m
Crystals $(\text{Pb}_y\text{Sn}_{1-y})_2\text{P}_2\text{S}_6$	0,05	-8,46	-1,48	2,24	5,7
	0,1	-8,33	-1,55	2,35	5,4
	0,2	-7,81	-1,26	2,15	6,2
	0,3	-6,70	-1,04	1,58	6,4
	0,4	-5,96	-0,86	1,30	7,0
	0,6	-6,96	-0,56	0,85	12,4
	0,8	-8,67	-0,57	0,86	15,3
$\text{Sn}_2\text{P}_2(\text{S}_{1-x}\text{Se}_x)_6$	0	-7,2	-1,41	2,35	5,1
	0,1	-7,36	-1,42	2,36	5,2
	0,3	-8,5	-1,38	2,38	6,3
	0,8	-7,2	-1,33	2,44	5,4
	1	-6,9	-1,27	2,35	5,4
$(\text{Pb}_y\text{Sn}_{1-y})_2\text{P}_2\text{Se}_6$	0,05	-5,2	-1,43	2,33	3,6
	0,2	-4,2	-1,40	2,21	3,0
	0,35	-6,2	-1,11	1,94	5,6
	0,8	-6,3	-0,74	1,35	8,5
	1	-7,8	-0,68	1,26	11,5

in the anionic sublattice in $\text{Sn}_2\text{P}_2(\text{S}_x\text{Se}_{1-x})_6$ crystals does not change essentially, neither the deformational potential D_g , nor m coefficient values.

Conclusions

The experimental studies of external hydrostatic pressure effect upon the fundamental absorption edge in $\text{Sn}_2\text{P}_2(\text{S}_x\text{Se}_{1-x})_6$, $(\text{Pb}_y\text{Sn}_{1-y})_2\text{P}_2\text{S}_6$ and $(\text{Pb}_y\text{Sn}_{1-y})_2\text{P}_2\text{Se}_6$ crystals were performed. It is shown experimentally that in $\text{Sn}_2\text{P}_2(\text{S}_x\text{Se}_{1-x})_6$ solid solutions pressure, along with the energy gap shrinkage, results in the decrease of the characteristic energy W , indicating the structural ordering of the crystals at hydrostatic compression. In the crystals under investigation the decrease of E_g^α with temperature is shown to be due mostly to the electron-phonon interaction. The increase of Pb concentration in $(\text{Pb}_y\text{Sn}_{1-y})_2\text{P}_2\text{S}_6$ and $(\text{Pb}_y\text{Sn}_{1-y})_2\text{P}_2\text{Se}_6$ crystals results in the enhancement of the electron-

phonon interaction and to the decrease of the deformation potential D_g of the energy gap. The isomorphous substitution of S by Se in the row of $\text{Sn}_2\text{P}_2(\text{S}_x\text{Se}_{1-x})_6$ solid solutions does not affect significantly the electron-phonon interaction value and D_g value. For $(\text{Pb}_y\text{Sn}_{1-y})_2\text{P}_2\text{S}_6$ ($0 \leq y \leq 0,10$) and $\text{Sn}_2\text{P}_2(\text{S}_x\text{Se}_{1-x})_6$ ($0 \leq x \leq 0,20$) solid solutions at the temperature $T = 296\text{K}$ the external pressure effect causes the second-order phase transition from the ferroelectric to the paraelectric phase. From the obtained results of temperature and pressure studies of the absorption edge for these compositions the pressure coefficients of of the phase transition temperature shift $\left(\frac{dT_0}{dp} \right)$ are calculated. The obtained $\frac{dT_0}{dp}$ values are in good agreement with the results of the direct studies of the phase p, T -diagrams.

References

1. Slivka A.G., Gerzanich E.I., Studenyak I.P. et.al. Ukr. Journ.Phys. **32** (1987) 1819 (in Russian).
2. Guranich P.P., Gerzanich E.I., Slivka A.G., Shusta V.S. Ukr. Journ.Phys. **35** (1990) 196 (in Russian).
3. Shusta V.S., Gerzanich E.I., Slivka A.G. et.al. Ukr. Journ.Phys. **37** (1992) 561 (in Russian).
4. Guranich P.P., Gerzanich E.I., Slivka A.G. et.al. Ferroelectrics **132** (1992) 173.
5. Shusta V.S., Gerzanich E.I., Slivka A.G. et.al. Ferroelectrics **145** (1993) 61.
6. Slivka A.G., Gerzanich E.I., Shusta V.S., Guranich P.P. Izv. Vus. RAN, ser.Phys. **9** (1999) 23 (in Russian).
7. Gurzan M.I., Buturlakin A.P., Gerasimenko V.S. et.al. Fiz.Tv.Tela **19** (1977) 3068- (in Russian).
8. Gerzanich E.I., Slivka A.G., Guranich P.P. et.al. Nauk.Visn UzhNU, ser.Phys. **6** (2000) 36 (in Ukrainian).
9. Cody G.D., Tiedje T., Abeles B. et.al. Phys.Rev.Letters **47** (1981) 1480-1483.
10. Slivka A.G., Gerzanich E.I., Guranich P.P., Shusta V.S. Ferroelectrics **103** (1990) 71.
11. Fridkin V.M. Ferroelectrics–semiconductors. Moscow "Nauka" (1976) 408p. (in Russian).
12. Shusta V.S., Guranich P.P., Gerzanich E.I. et.al. Ukr. Journ. Phys. **40** (1995) 959 (in Ukrainian).